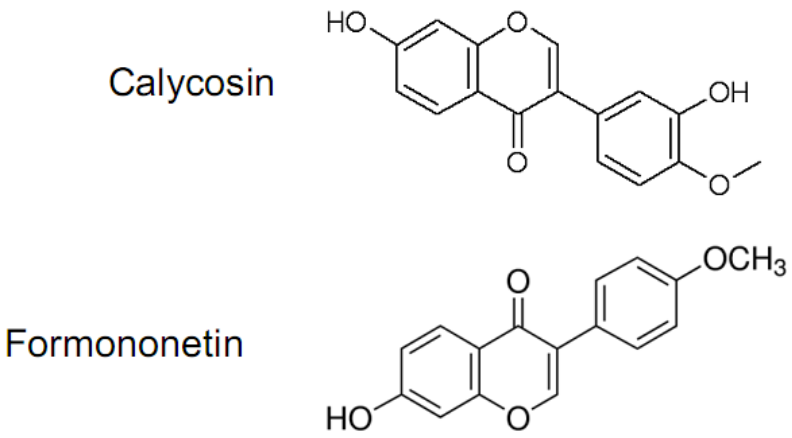

Figure S1. The chemical structure of the natural compounds formononetin and calycosin.

A. The spectra of chiral column analysis of water extracts of *Astragalus membranaceus*.

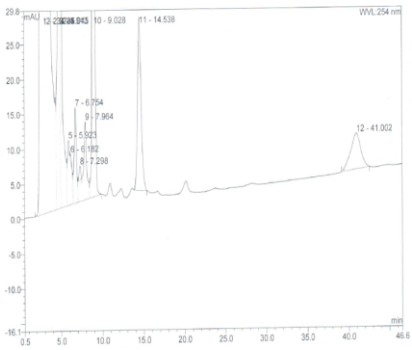

No.	Ret.Time (min)	Height (mAU)	Area (mAU*min)	Rel.Area (%)	Type
1	2.87	460.27	174.34	34.18	MB*
2	3.28	539.94	196.90	38.61	BMB*
3	4.91	299.35	53.21	10.43	M*
4	5.04	310.03	42.20	8.27	M*
5	5.92	2.73	0.58	0.11	BMB*
6	6.75	8.02	1.54	0.30	BMB*
7	7.96	5.57	1.06	0.21	BMB*
8	9.03	70.61	20.40	4.00	BMB*
9	14.54	24.76	12.46	2.44	BMB*
10	**41.00**	**5.08**	**7.29**	**1.43**	**BMB***
Total		1726.40	510.00	100.00	

B. The spectra of chiral column analysis of formononetin.

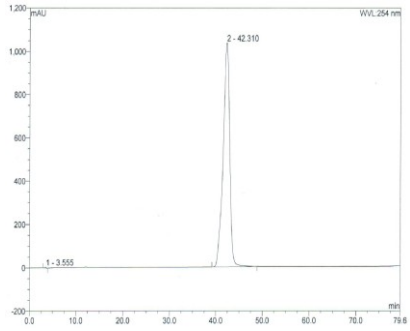

No.	Ret.Time (min)	Height (mAU)	Area (mAU*min)	Rel.Area (%)	Type
1	3.56	4.03	1.17	0.07	BMB*
2	**42.31**	**1034.14**	**1722.29**	**99.93**	**BMB***
Total		1038.17	1723.45	100.00	

Figure S2. The HPLC analysis of the water extract of *Astragalus membranaceus* (A) and formononetin (B).

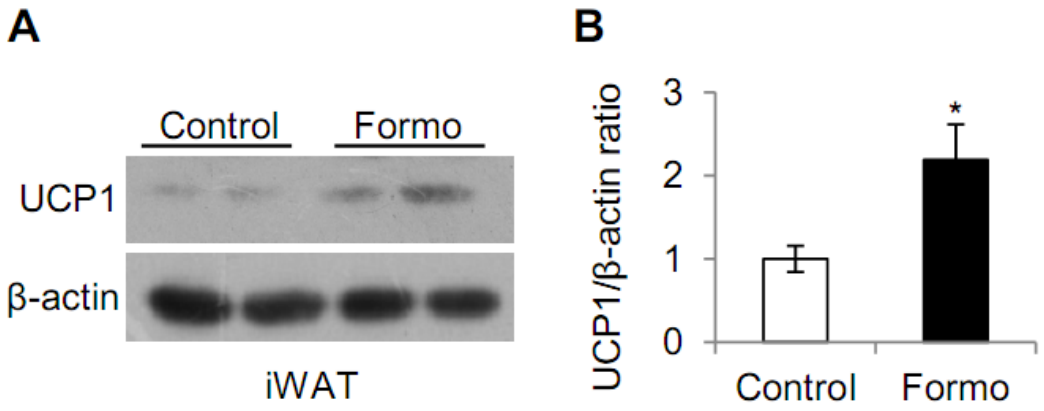

Figure S3. The UCP1 expression was detected in the inguinal adipose tissues. Western blot analysis of UCP1 in the inguinal white adipose tissue (iWAT, A) and densitometric analysis of the relative abundance of UCP1 (B) (n = 5), β-actin was adopted as an internal standard to control for unwanted sources of variation, the ratio of UCP-1 expression in BAT was normalized to β-actin (control). Data represent mean ± SEM, the experiments had been repeated three times, *$p<0.05$.

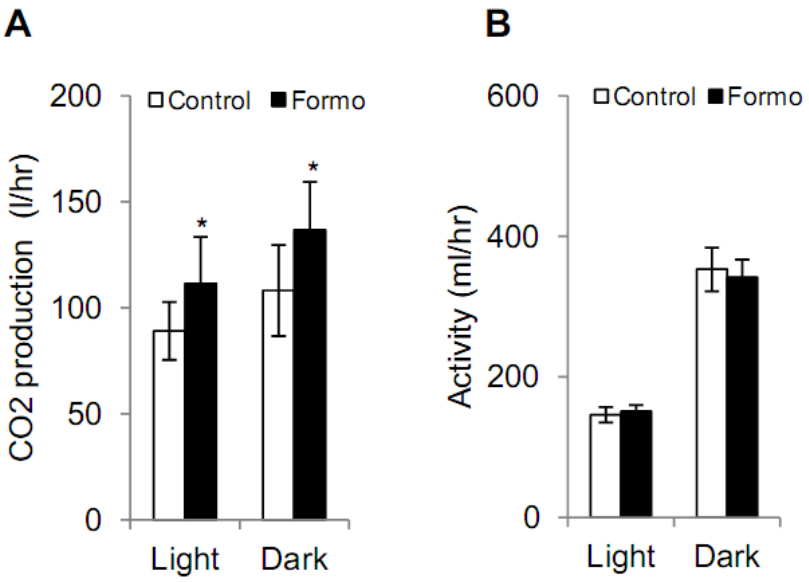

Figure S4: Eight-week-old C57BL/6J male mice were fed a high fat diet for 8 weeks to become obese and then treated with the vehicle or formononetin for 8 weeks, followed by analysis of (A) CO_2 production, (B) activity. (n=5). Data represent mean ± SEM, the experiments had been repeated three times, *$p<0.05$.

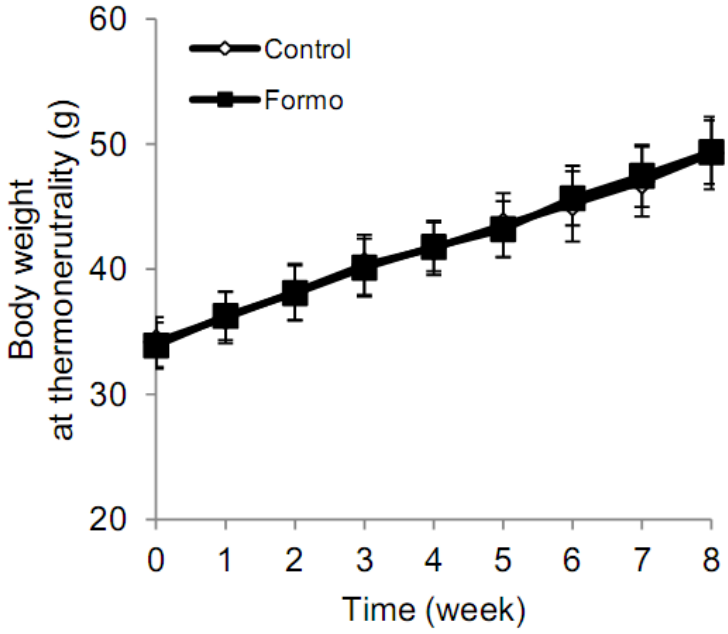

Figure S5: Eight-week-old C57BL/6J male mice were fed a high fat diet for 8 weeks to become obese and then treated with the vehicle (control) or formononetin for 8 weeks at thermonerutality (n = 6 mice).

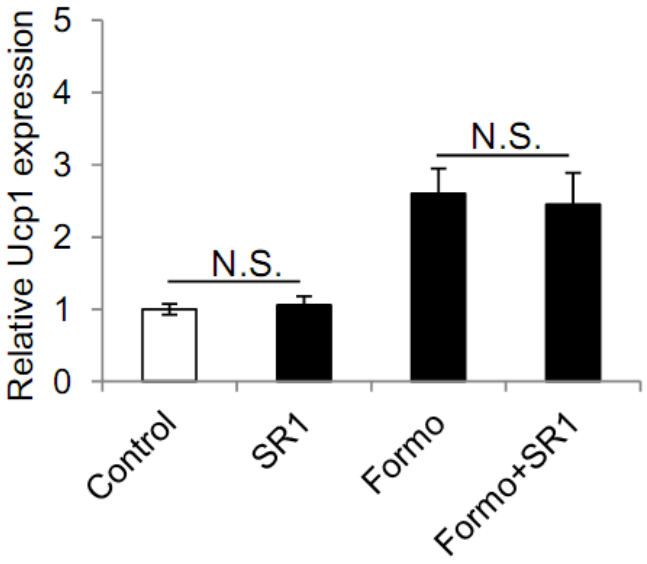

Figure S6: The synergistic effect of AhR inhibitor StemRegenin 1 (SR1) and formononetin on *Ucp1*'s expression (n = 5). For quantitative RT-PCR experiments, 18S ribosomal RNA was adopted as an internal standard to control for unwanted sources of variation. The *ucp1* gene's average mRNA expression was normalized to the blank control (baseline). Data represent mean ± SEM, the experiments had been repeated three times, *$p<0.05$.

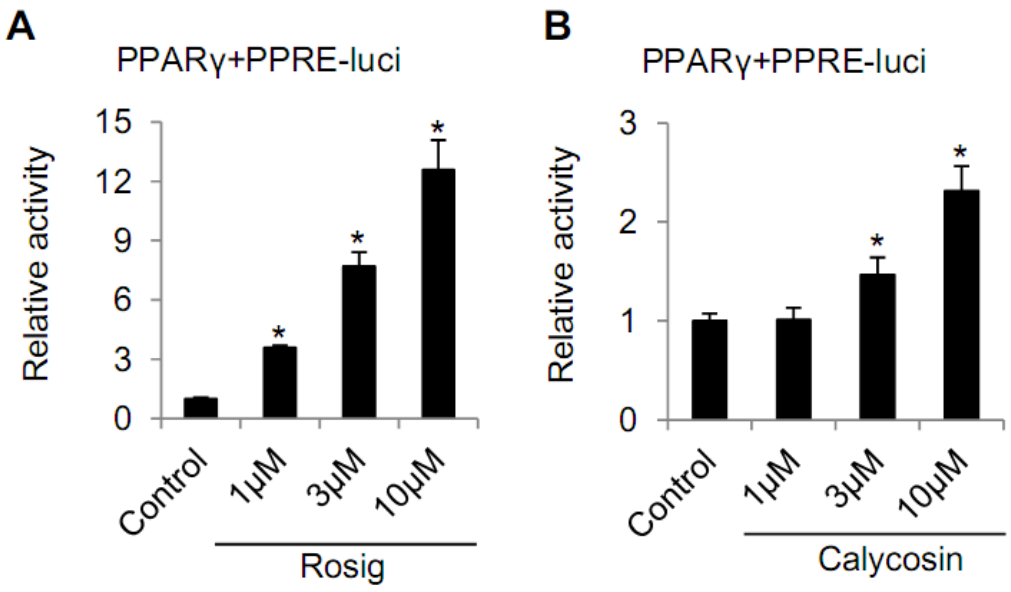

Figure S7: Rosglitazone (A) and calycosin (B) dose dependently promoted luciferase activity in COS7 cells transfected with PPARγ and PPRE-luciferase plasmids (n = 5). The luciferase activity was normalized to the blank control as baseline. Data represent mean ± SEM, the experiments had been repeated three times, *$p<0.05$.

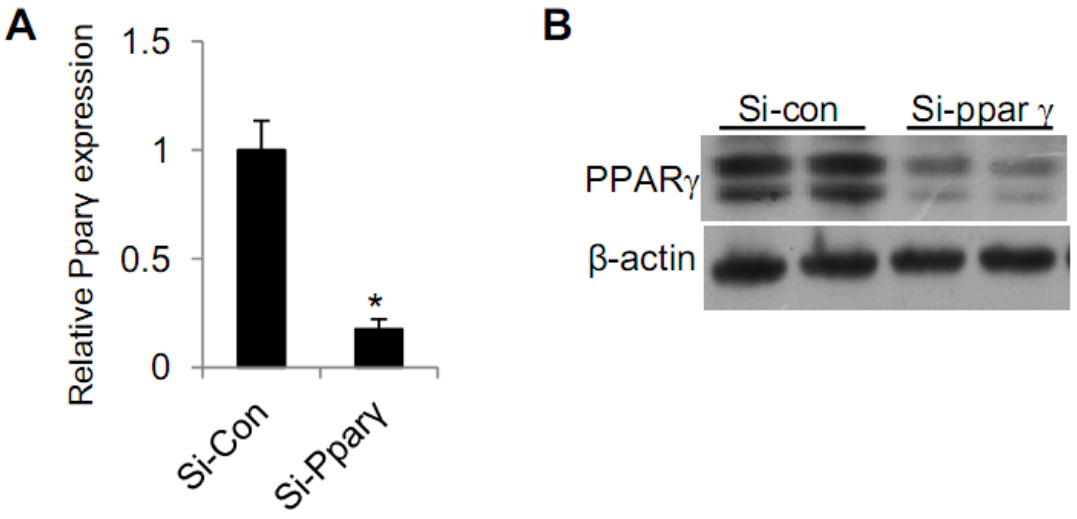

Figure S8: The mRNA (A) and protein (B) expression of *Pparγ* in siRNA knockdown of *Pparγ* in primary inguinal adipocytes (n = 5). For quantitative RT-PCR experiments, 18S ribosomal RNA was adopted as an internal standard to control for unwanted sources of variation. The *Pparγ* gene's average mRNA expression was normalized to the blank control (baseline). Data represent mean ± SEM, the experiments had been repeated three times, *$p<0.05$.

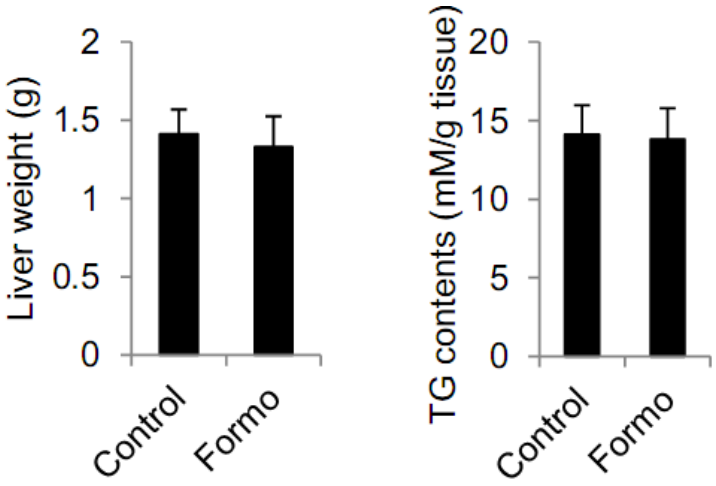

Figure S9. The liver tissue weight (left) and TG contents in liver (right) in control mice and formononetin treated mice (n = 5). Data represent mean ± SEM, the experiments had been repeated three times, *p<0.05.